Chinese Journal of Aeronautics, (2014),27(5): 1318–1326

Chinese Society of Aeronautics and Astronautics
& Beihang University

Chinese Journal of Aeronautics

cja@buaa.edu.cn
www.sciencedirect.com

A new vibration mechanism of balancing machine for satellite-borne spinning rotors

Wang Qiuxiao *, Wang Fei

College of Mechanical Engineering, Chongqing University, Chongqing 400030, China

Received 9 September 2013; revised 6 December 2013; accepted 15 April 2014
Available online 19 August 2014

KEYWORDS

Rotational unbalance;
Satellite-borne rotor;
Separation of static unbalance and couple unbalance;
Vertical balancing machine;
Vibration measurement

Abstract The centrifugal force and overturning moment generated by satellite-borne rotating payload have a significant impact on the stability of on-orbit satellite attitude, which must be controlled to the qualified range. For the satellite-borne rotors' low working revs and large centroidal deviation and height, and that the horizontal vibration produced by centrifugal force is not of the same magnitude as the torsional vibration by overturning moment, the balancing machine's measurement accuracy is low. Analysis shows that the mixture of horizontal vibration and torsional vibration of the vibrational mechanism contribute mainly to the machine's performance, as well as the instability of vibration center position. A vibrational mechanism was put forward, in which the horizontal and torsional vibration get separated effectively by way of fixing the vibration center. From experimental results, the separation between the weak centrifugal force signal and the strong moment signal was realized, errors caused by unstable vibration center are avoided, and the balancing machine based on this vibration structure is able to meet the requirements of dynamic balancing for the satellite's rotating payloads in terms of accuracy and stability.

1. Introduction

The rotating antenna mechanisms, such as the microwave scanning radiometer and the microwave imager, are important remote sensing instruments as well as primary payloads in the meteorological and oceanographic satellites,[1,2] generally working in the mechanical rotary scanning mode. If the inertial force itself within the antenna scanning mechanism cannot counteract internally, huge trouble could be caused to satellites suspended in space with interference torque generated by the rotation acting on the satellite body.[3–6] Firstly, the aroused vibration in the satellite will directly affect the image pixel registration accuracy and reduce geographic positioning accuracy due to image distortion in the detection equipment, the satellite's technical working index is lowered in consequence; Secondly, large unbalanced force and moment lead to the reduction of accuracy and stability of the satellite's attitude, so that satellites has to constantly adjust itself in order to maintain the normal operation at the cost of increasing the fuel and electricity consumption, which could shorten the working life and degrade the operational reliability. Obviously, it is required for rotating antenna elements to be balanced in

* Corresponding author. Tel.: +86 23 65429037.
E-mail address: wqxiao1963@163.com (Q. Wang).

Peer review under responsibility of Editorial Committee of CJA.

ELSEVIER Production and hosting by Elsevier

http://dx.doi.org/10.1016/j.cja.2014.08.001

advance on the ground, which has an important significance to satellites' stable operation in orbit.

Brought from rotating antenna parts' processing errors and asymmetric integration assembly work, the dynamic unbalance will generate a certain amount of centrifugal force and the moment of inertia. In the balancing control for an antenna, it needs to be installed in a vertical double-plane balancing machine, so as to simulate working conditions in orbit for test. According to the test results, the mass distribution of the rotating parts gets improved by trim and correction at specific locations, minimizing the deviation between the mass center, inertial principal axis and the rotation axis, adjusting the unbalance to be within the control target range.

Horizontal balancing machines have achieved good results in many aspects, e.g., self or automatic balancing technology,[7,8] kinetic model optimization,[9,10] corresponding balancing theories at different working speeds,[11,12] multi-plane separation techniques,[13] optimization algorithm.[14,15] In comparison, many key techniques are not mature yet at present in the vertical hard bearing double-plane dynamic balancing machine, of which the separation ratio is unsatisfactory and the measurement accuracy is low. Lee and Warkotsch use a frame-style vibration structure to detect vibration signals through sensors mounted on different planes of the rotor.[16,17] In the study of vertical automatic balance, Royzman and Drach created automatic balancing units made as hollow rotor partially filled with liquid, and in their units passive balancing is used and those units are direct controllers as their sensitive element produces force enough to balance rotor;[18] Rajalingham and Bhat presented an automatic balancer consisting of several balancing balls which are guided to move in a circular track. In the study the suitability of a two-ball automatic balancer to balance the residual unbalance in a vertical rotor is investigated, and the nonlinear analysis revealed that under certain conditions, the system ultimately settles down to the balanced steady state and thereby balance the residual unbalance in a vertical rotor completely.[19] Ferraris, Andrianoely, Berlioz et al. investigated the balancing procedure of a rotary refrigerant compressor subjected to fairly well-known eccentric masses and to a cylinder pressure force. Particular attention is paid to the influence of pressure force on the response of the compressor. It demonstrates that cylinder pressure plays a negligible role in the case of the rotary machine presented here, but must be taken into account when high pressure and weak bearing characteristics are combined.[20] Hredzak and Guo proposed a new type of electromechanical balancing device that can be used for active compensation of variable unbalance of a rotational machine, the main advantage of which is in its capability to reduce rotational unbalance in applications where the value and position of unbalance is variable.[21]

In the study of spaceborne rotor balancing, Wilson and Mah presented an approach for automatic balancing and intelligent fault tolerance and the research focused on the automatic on-line balancing and the associated fault tolerance. In the automatic balancing system, feedback from sensors measuring rotor motions or forces is used to drive active counterweights to null the unbalance and resulting vibrations.[22] To reduce two types of unbalances in the spinning rocket vehicles and satellites in the atmosphere, static and dynamic unbalances, Sethunadh and Mohanlal developed a novel virtual instrument-based measurement system which consists of a single acquisition board and a power supply unit.[23] Brusa and Zolfini carried out a numerical and experimental investigation on the dynamic behaviour of a fixed multi-body fast-spinning rotor in order to validate the design approach proposed for a spacecraft.[24] However, satellites with multi-body rotors as a whole are usually balanced through air-bearing spacecraft simulators. Schwartz and Wiener address the problem of statically and dynamically balancing a satellite with antenna rotor mounted supported on its own bearings and driven by a motor in the satellite body.[25,26]

The study found that large height and centroidal deviation give rise to nonlinear deformation of the antenna on one hand; therefore, there exists large test error; on the other hand, since the working rev is low, the vibration signals are poor, and the signals of torque during the test interfere with the signals of centrifugal force severely. To meet the requirements of high precision for the rotating antenna balance, sufficient separation is necessary between the two components so as to reduce the coupling interference. Accordingly, the reflection in the mechanical system is the separation of the horizontal and torsional vibration aroused by the rotor unbalance. The effective separation between the two is directly related to the measurement accuracy, which is the key technique of vertical double-plane balancing machines and also the technical difficulties that has long been not resolved well.

The objective of this paper is to investigate the vibration mechanism of the balancing machine for the single satellite-borne rotor's balancing in advance on the ground. According to the analysis of the vibration structures of the existing vertical balancing machines and combined with the properties of satellite-borne rotating antennas, a new type of vibration mechanism is presented, then the vibration model is established and the structural parameters is researched. Finally, experiments are provided for the verification of the correctness of the separation principle of horizontal vibration and torsional vibration, and the performance of the balancing machine based on this new vibration mechanism.

2. Unbalance of satellite-borne rotating antenna

Shown in Fig. 1, the satellite-borne antenna mechanism consists of the reflector, bracket, rotating cylinder and other components. The cylinder is driven by a built-in motor and connects with the main satellite body at the bottom. Due to long-term use under the vacuum of space, the oil-bearing structure is used between the cylinder and the stator. To ensure the safety of work, the mechanism typically operates at about 10–50 r/min.

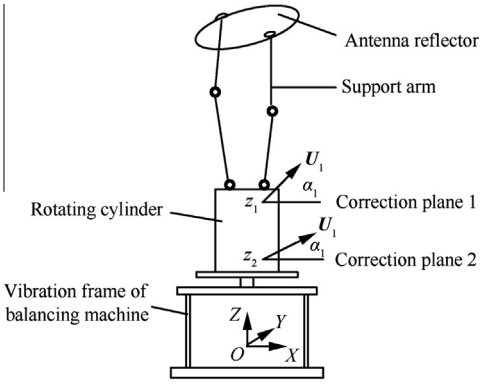

Fig. 1 Unbalance test for satellite-borne rotating antenna.

In general, the centroidal deviation and height is large in the satellite-borne rotating payloads with asymmetric structure. Thereinto, the cap-shaped antenna reflector deviates from the axis of rotation and has a considerable height from the foot of the supporting shaft. A rather great overturning moment is generated as a result when the rotating payload is scanning. So, in the sensor detecting process, the signal strength of the overturning moment produced by unbalance is much greater compared to that of the centrifugal force.

This kind of satellite-borne payloads are generally of low rigidity, and in order to achieve the high measurement accuracy of unbalanced force and moment in the condition of large-size and low speed, first of all, the balancing test structure of vertical double-plane and hard bearing is adopted. The test installation is shown in Fig. 1. In the unbalance detection for satellite-borne rotating parts, two ways are employed in general: one is the balancing of the components of products, which are directly installed on the flange of the balancing machine's spindle and driven by the spindle when measured; the other is the balancing of the whole products, in which the balancing machine's spindle is fixed and the rotor is driven by the built-in motor of the product. In the second case, the balancing machine seen as the satellite body to simulate the working state in orbit, the unbalance would be reflected by the vibrational mechanism of the dynamic balancing machine.

When performing the balancing correction, the trim should be operated just on two planes of the rotating cylinder for the structural reason. The synthetic unbalance $\boldsymbol{U}$ of the entire antenna assembly is equivalent to the unbalance $\boldsymbol{U}_1$ on the upper plane z_1 and $\boldsymbol{U}_2$ on the lower plane z_2, namely

$$\begin{aligned}\boldsymbol{U} &= \boldsymbol{U}_1 + \boldsymbol{U}_2 \\ &= (U_1\cos\alpha_1 + U_2\cos\alpha_2)\boldsymbol{i} + (U_1\sin\alpha_1 + U_2\sin\alpha_2)\boldsymbol{j}\end{aligned} \tag{1}$$

where α_1, α_2, U_1, U_2 are respectively the corresponding phase angles and magnitudes of $\boldsymbol{U}_1$ and $\boldsymbol{U}_2$, and $\boldsymbol{i}$, $\boldsymbol{j}$ are unit vectors of X-axis and Y-axis. So, the synthetic couple unbalance V is expressed as

$$\begin{aligned}\boldsymbol{V} = \boldsymbol{k}\times(I_{xz}\boldsymbol{i} + I_{yz}\boldsymbol{j}) = \boldsymbol{k}\times[(U_1z_1\cos\alpha_1 + U_2z_2\cos\alpha_2)\\ \boldsymbol{i} + (U_1z_1\sin\alpha_1 + U_2z_2\sin\alpha_2)\boldsymbol{j}]\end{aligned} \tag{2}$$

where I_{xz} and I_{yz} are respectively the rotating body's product of inertia relative to the coordinate system $OXYZ$, and $\boldsymbol{k}$ is the unit vector of Z-axis.

All the above analysis shows that the dynamic unbalance could be described with two kinds of components, the static unbalance $\boldsymbol{U}$ and the couple unbalance $\boldsymbol{V}$. According to the structure parameters of the vibration system and sensor signals, through appropriate calibration for the electrical test system to establish relationships between electrical and mechanical systems, the unbalance distributed on correction planes is quickly and accurately considered by Eqs. (1) and (2), then the trimming would be carried on.

3. Analysis of general vibration mechanisms

3.1. Frame-style vibration mechanism

The positions of the sensors in the frame-style vibration mechanism are shown in Fig. 2. c is the mass center of the spindle system (the test pieces included), and assumed to be between the upper sensor and the lower sensor(similarly in other cases). F_1 and F_2 are the concentrated unbalanced force of the two correction planes, which are in the same phase to facilitate the discussion. L_1 is the distance between F_1 and F_2 vertically, L_2 is the distance between F_2 and sensor 1 vertically, L_3 is the distance between sensor 1 and X_1-axis vertically, L_4 is the distance between sensor 2 and X_1-axis vertically, and L_5 is the distance between point O_1 and X_1-axis vertically. In the vibration, the spindle system generates horizontal displacement x_1 by the unbalance forces F_1 and F_2, as a result, the mass center moves from c to c'; meanwhile, the spindle system rotates around c' with the rotation angle θ_1 under the action of the unbalanced moments $F_1(L_1 + L_2 + L_3)$ and $F_2(L_2 + L_3)$. The intersection of the spindle axis and the rotation axis O_1 is the vibration center.

Let the two sensor measurement values be N_1 and N_2, then the relationship between the values and the unbalanced forces is

$$\begin{cases} N_1 = \dfrac{F_1(L_1 + L_2 + L' + \lambda) + F_2(L_2 + L' + \lambda)}{L' + 2\lambda} \\ N_2 = \dfrac{F_1(\lambda - L_1 - L_2) + F_2(\lambda - L_2)}{L' + 2\lambda} \end{cases} \tag{3}$$

where $L' = L_3 + L_4$, $\lambda = k_2/L_5k_1$, and k_1 and k_2 are the horizontal and torsional rigidity of the vibration mechanism respectively.

With Fig. 2 and the Eq. (3), the centrifugal force and the moment are detected by sensors at the same time, when the horizontal signal and the rotational signal are mixed with the result of severe superimposed interference. What's more, sensors should be resolved to obtain the unbalance of each correction plane, and if there exist performance errors in sensors, mutual coupling effects would result in the amplification of the measurement errors of the unbalances, which is closely related to the sensors coupling degree. Therefore, it is not conducive to improve the unbalance separation accuracy of each correction plane, reducing the effect of the balance correction at a time.

Supposing that an existing unbalance U' is at the height of h_1 in the test antenna, the change of the displacement of the spindle system during the measurement is indicated in Fig. 3.

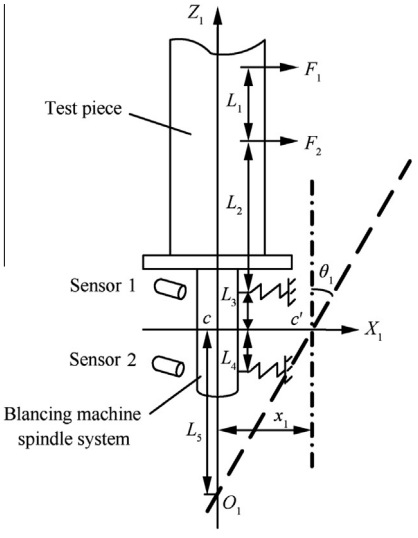

Fig. 2 Frame-style measurement diagram.

where x_1, x_1' are respectively the corresponding displacements of the locations of the mass center and the sensor, then

$$\begin{cases} x_1' = x_1 + \Delta x \\ \Delta x = L_3\theta_1 = \varphi(U', h_1) \end{cases} \tag{4}$$

Seen from Eq. (4), Δx is the linear function[13] of variable U', h_1. The torsional stiffness is much larger than the horizontal stiffness and the rotation angle θ is rather small, as a result, $\Delta x << x_1$; from the structural point of view, the rotating part is of greater height, so that while h_1 is of small amount of change, there is little change of Δx if the unbalance U' is of rather height (namely h_1 is large) according to Eq. (4). These two factors result in insensitivity of sensors to the unbalances in high positions, so, vibration mechanisms of this type are not suited to satellite-borne rotating antennas with the centroid deviation aloft.

Since the general vibrating motion of the system can be considered as the synthesis of the horizonal motion along with the mass center and the torsional motion around the mass center, there should be a point that is determinate in the vibration system (or the extension) and called the vibration center as shown in Fig. 2. In order to improve the height of the vibration center, Li optimized the design on the basis of the frame-style mechanism.[27] However, due to the change of test pieces, speed fluctuation and the instability of the vibration center by long-term operating, the actual mechanical separation ratio will change, the permanent calibration is unable to achieved, and the plane separation error occurs after subsequent electrical measurements. Therefore, this type of applications has great limitations when used for the spinning antennas.

In addition, to measure the static unbalance and the couple unbalance at the same time, k_1 and k_2 should be on the same order of magnitude; however, it is hard to achieve in structural design for the frame-style mechanism using the spring-plate to reflect the static and couple unbalances simultaneously.

3.2. Bi-directional vibration mechanism

In this type of mechanisms the sensor installation is shown in Fig. 4. Also, the coordinate system is established with the mass center of the spindle system as the origin. To simplify the description, it is assumed that the test body contains concentrated unbalanced force on a single plane, namely $F_3 = mr\omega^2 \cos(\omega t)$. The perpendicular distance from mass center c to the sensor 1 is a, the perpendicular distance from the unbalance F_3 to the sensor 2 is h_2, and the horizontal distance from the sensor 2 to the rotation axis is b. k_3 and k_4 are the horizontal and torsional rigidity of the vibration mechanism respectively.

During vibrating process, the mass center c has a horizontal offset x_2, while the rotation angle of the spindle system around the mass center is θ_2, then

$$\begin{cases} x_2 = \dfrac{F_3}{k_3} \\ \theta_2 = \dfrac{(a+h_2)F_3}{k_4 b^2} \end{cases} \tag{5}$$

and the corresponding displacement of the installation location of sensor 1 is

$$x_2' = \left[\frac{1}{k_3} + \frac{a(a+h_2)}{k_4 b^2}\right] F_3 \tag{6}$$

so, the perpendicular distance from the vibration center O_2 to sensor 1 is

$$L = \frac{x_2'}{\theta_2} = \frac{k_4 b^2}{a+h_2} + k_3 a \tag{7}$$

On the one hand, the position of the mass center of the spindle system will generally change as the test pieces are different, on the other, the installation of the sensor 1 will bring about the positional deviation because the horizontal mechanical part of this type of testing mechanisms cannot be well identified. According to Eqs. (5)–(7), the uncertainties of a, h_2 and $a + h_2$ caused by the above two factors, are likely to cause the error of rotation angle θ_2 and the displacement x_2' of the installation location of the sensor 1; moreover, the instability of L, the position of the vibration center, could result in the calibration error of the measurement system eventually as well. Therefore, the vibration mechanisms based on this principle always have unsatisfactory stability, and is unable to meet the high-precision requirement of satellite-borne rotating payloads.

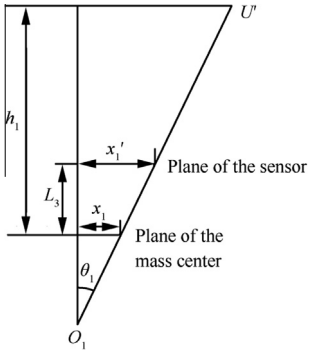

Fig. 3 Change of displacement of spindle system during measurement.

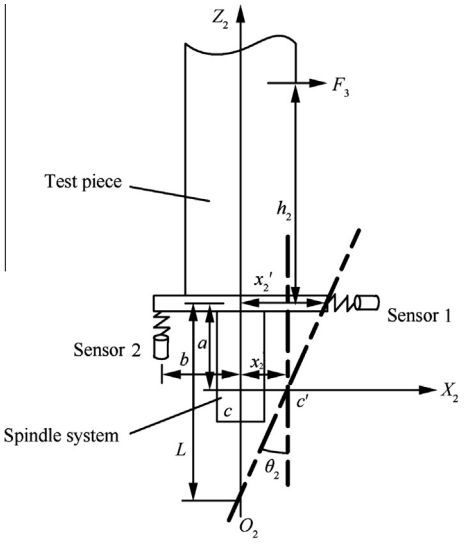

Fig. 4 Bi-directional measurement diagram.

4. Study of a new vibrational mechanism

Fig. 5 shows the originally designed principle prototype of the vibrational mechanism, which has achieved good performance. However, the spindle system of the structure is carried by two cross spring rods, for which it is hard to meet the load requirements under the conditions of large size and quality. Thus, floating phenomenon may appear in the course of rotation, reducing the measurement stability.

In the research of this field, the vibration mechanism of the typical balancing machines represented by E series from Schenck of Germany, adopts a flexing member as the torsional fulcrum, which is similar to the cross structure s- shown in Fig. 5 in principle but is of high price and unsatisfactory economic efficiency.

Aimed at the problems existing in the conventional mechanisms, combined with the cross-shaped swing frame theory, a new vibration mechanism is proposed to meet the speciality of satellite-borne rotating payloads.

4.1. Vibration mechanism

Fig. 6 shows the diagram of the new type of dynamic balancing vibration mechanism, in which the whole structure is connected to the base trough the left and right horizontal spring-plates and the spindle system (including test piece) coordinates with the torsional shaft through the support. Under the action of the centrifugal force generated by the unbalance in the test piece, the spindle system, support and torsional shaft make a horizontal vibration along with the support board when rotating, meanwhile the spindle system and the support swing around the torsional shaft by the overturning moment. This vibration system is limited to the above two degrees of freedom.

In the vibration mechanism, the spindle system is mounted on the torsional shaft. On the one hand the position of the torsional center is determined, on the other hand the carrying capacity of the spindle is improved so as to meet the measurement requirements of antenna rotors with large weight. The horizontal vibration resulting from the centrifugal force is embodied in the horizontal spring-plate, while the torsional vibration in the torsional spring-plate is detected respectively by the horizontal sensor 1 and the vertical sensor 2. In the establishment of dynamic model, the torsional center is set as the reference origin. Therefore, the measurement of the unbalance is not concerned with the stability of the position of the vibration center, which avoids the errors always appearing in constant vibration mechanisms.

And, since the overturning moment of the satellite-borne antenna is larger, that is, the couple unbalance is much greater

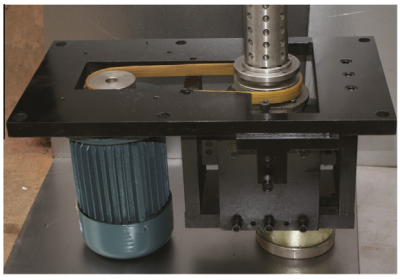

Fig. 5 Cross-shaped swing frame.

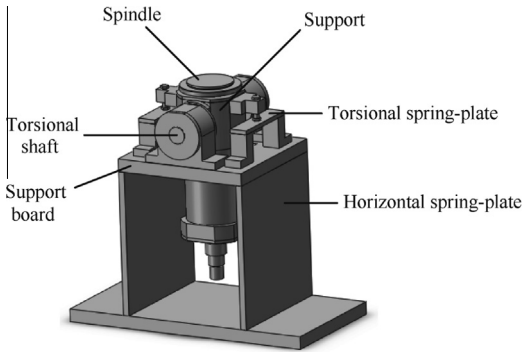

Fig. 6 Separation mechanism of static and couple unbalance.

than the static unbalance, in order to ensure the signal strength of the sensor, the horizontal spring-plate's thickness cannot be too large, which is in contradiction with that the vibration mechanism should have a large rigidity to meet the large weight of the antennas. Therefore, the optimization design is necessary for the vibration characteristics of the mechanism to achieve the optimal performance via the analysis software like Ansys.

4.2. Vibration of analysis

In Fig. 7, the spindle system shifts and tilts under the static and couple unbalances, and O_3 and O_3' are the corresponding positions of the torsional centers before and after the deflection. The coordinate system $O_3X_3Y_3Z_3$ is set at the origin of the center O_3 of the torsional shaft while the $O_4X_4Y_4Z_4$ at the mass center O_4 of the spindle system, and the orientation is shown in the figure. The sensors are used to measure the signals of the horizontal and torsional motions. l is the distance from sensor 2 to the axis of the spindle with the angular velocity ω, and the distance from O_4 to the torsional shaft axis is H in the vertical direction. The rigidity of the left horizontal spring-plates is k_5, the same as the right one, and the rigidity of the torsional spring-plate is k_6. u_1 and u_2 are assumed to be the unbalance of the two correction planes, and the phase angles are α_1 and α_2 accordingly. θ is the rotation angle of the spindle system, and x is the horizontal displacement of the translational body.

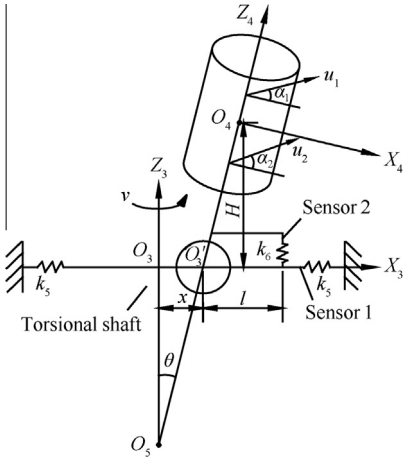

Fig. 7 Model of vibration system.

u_1 and u_2 can be described by the static unbalance U and the couple unbalance V, whose phase angles are α_3 and α_4 respectively. Let F be the centrifugal force and T the overturning torque, so $F = U\omega^2\cos(\omega t + \alpha_3)$, $T = V\omega^2\cos(\omega t + \alpha_4)$. Ignoring the gravity torque and the system damping, the differential equation of the vibration system is

$$\begin{cases} M\ddot{x} + mH\ddot{\theta} + 2k_5 x = F \\ J\ddot{\theta} + m(\ddot{x} + H\ddot{\theta})H + k_6 l^2\theta = Fh + T \end{cases} \tag{8}$$

where M is the total mass, m the mass of the rotational body, J the inertia of moment of the rotational body about the rotation center, and h the vertical distance of the static unbalance from the torsional center O_3'.

Using Laplace transform, the Eq. (8) changes to be

$$\begin{cases} (Ms^2 + 2k_5)x(s) + mHs^2\theta(s) = F(s) \\ (Js^2 + mH^2s^2 + k_6l^2)\theta(s) + mHs^2x(s) = F(s)h + T(s) \end{cases} \tag{9}$$

Let $\omega_{n1} = \sqrt{\dfrac{2k_5}{M}}, \omega_{n2} = \sqrt{\dfrac{k_6l^2}{J + mh^2}}$ respectively the natural frequencies of the horizontal motion and the torsional motion of the vibration system, then the response equation obtained from Eq. (9) is

$$\begin{cases} M(\omega_{n1}^2 - \omega^2)x(\mathrm{j}\omega) - mH\omega^2\theta(\mathrm{j}\omega) = F(\mathrm{j}\omega) \\ (\omega_{n2}^2 - \omega^2)(J + mH^2)\theta(\mathrm{j}\omega) - mH\omega^2x(\mathrm{j}\omega) \\ = F(\mathrm{j}\omega)h + T(\mathrm{j}\omega) \end{cases} \tag{10}$$

Because the system is a hard supporting structure, i.e. $\omega_{n1} \gg \omega$, $\omega_{n2} \gg \omega$, Eq. (10) is simplified to be

$$\begin{cases} 2k_5x = U\omega^2\cos(\omega t + \alpha_3) \\ k_6l^2\theta = U\omega^2\cos(\omega t + \alpha_3) + V\omega^2\cos(\omega t + \alpha_4) \end{cases} \tag{11}$$

The two corresponding values F_{n1}, F_{n2} of the sensors are

$$\begin{cases} F_{n1} = k_5x \\ F_{n2} = k_6l\theta \end{cases} \tag{12}$$

So, the following equation can be obtained from Eqs. (11) and (12):

$$\begin{cases} U = \dfrac{2F_{n1}}{\omega^2\cos(\omega t + \alpha_3)} \\ V = \dfrac{F_{n2}l - 2F_{n1}}{\omega^2\cos(\omega t + \alpha_4)} \end{cases} \tag{13}$$

The equation above shows the relationship between the unbalance and the values of sensors, in which the sensor 1 is mounted in the position just corresponding to the torsional shaft's center and the static unbalance is reflected singly by the sensor 1, eliminating the interference by the couple unbalance and achieving mechanical separation between the horizontal signal and the torsional signal.

4.3. Parametric analysis

Eq. (8) is solved to be

$$\begin{cases} x = U\omega^2(k_2l^2 - J\omega^2 - m_1H^2\omega^2 + m_1Hh\omega^2)\cos(\omega t + \alpha_3) + m_1H\omega^4V\cos \\ \quad \times(\omega t + \alpha_4)/(2k_1 - m\omega^2)(k_2l^2 - J\omega^2 - m_1H^2\omega^2) - m_1^2H^2\omega^4 \\ \theta = U\omega^2(m_1H\omega^2 + 2k_1h - mh\omega^2)\cos(\omega t + \alpha_3) + (2k_1 - m\omega^2)\omega^2V \\ \quad \times\cos(\omega t + \alpha_4)/(2k_1 - m\omega^2)(k_2l^2 - J\omega^2 - m_1H^2\omega^2) - m_1^2H^2\omega^4 \end{cases} \tag{14}$$

In the equation above, the parameters are fixed except the parameters to be measured related to the unbalance and the mass center's position H of the spindle system. Generally, the mass center O_4 does not coincide with the torsional shaft's center O_3' (namely $H \neq 0$), so that the value of H changes with different test pieces. Therefore, the effect of the vibration system bears on not only the unbalances but also the test piece itself, which is not conducive to creating a strict proportion of the test system and the mechanical system.

Since the vibration mechanism is classified to be the hard bearing structure, and the natural frequency of vibration system is much larger than ω, Eq. (14) with the components containing ω^2 omitted turns into

$$\begin{cases} x = \dfrac{Uk_2l^2\omega^2\cos(\omega t + \alpha_3) + m_1HV\omega^4\cos(\omega t + \alpha_4)}{2k_1k_2l^2} \\ \theta = \dfrac{Uh\omega^2\cos(\omega t + \alpha_3) + V\omega^2\cos(\omega t + \alpha_4)}{k_2l^2} \end{cases} \tag{15}$$

For further simplification, the equation above is to be

$$\begin{cases} x = \dfrac{U\omega^2\cos(\omega t + \alpha_3)}{2k_1} \\ \theta = \dfrac{Uh\omega^2\cos(\omega t + \alpha_3) + V\omega^2\cos(\omega t + \alpha_4)}{k_2l^2} \end{cases} \tag{16}$$

This result is consistent with Eq. (11), in which it is clear that the effect of H is eliminated on the horizontal displacement x and the angle of rotation θ. So, this will ensure that the vibration effect structurally has nothing to do with the test piece and only the unbalance is relevant.

5. Performance test

To check the claimed performance of the prototype employing the new vibration mechanism, two independent experiments will be conducted: the mechanical separation principle experiment (couple unbalance interference on static unbalance), and the detection of U_{mar} (stability detection of minimum achievable residual unbalance).

5.1. Separation of horizontal vibration and torsional vibration

The deduction from Eqs. (11) and (12) is

$$\begin{cases} F_{n1} = \dfrac{U\omega^2\cos(\omega t + \alpha_3)}{2} \\ F_{n2}l = U\omega^2\cos(\omega t + \alpha_3) + V\cos(\omega t + \alpha_4) \end{cases} \tag{17}$$

Usually in the evaluation tests of performance in the balancing machine, the indication interference of the couple unbalance on the static unbalance is requested only on the single plane balancing machine. Since the couple unbalance is much larger than the static unbalance in the satellite-borne antenna, further observation is necessary to observe the interference from the couple unbalance especially at low revs. It is an experimental prototype in Fig. 8.

In Fig. 8, a standard testing rotor R should be fixed on the spindle's flange, of which the mass $M_{\mathrm{R}} = 47.6$ kg, the diameter $D = 100$ mm, and the height $H_{\mathrm{R}} = 510$ mm. The rotor R has eight testing surfaces 1–8 from low to high evenly with the space $\Delta h = 50$ mm. The distance from the testing surface 1 to the center of the rotational shaft is 150 mm, 8 testing holes

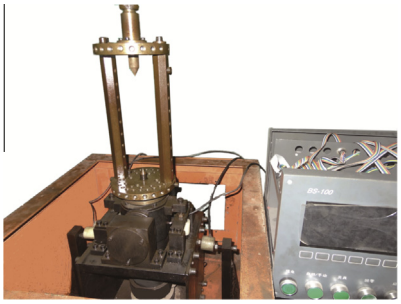

Fig. 8 Practical small-scale testing vibration mechanism.

is around each surface uniformly (requiring higher positioning accuracy), and the testing radius $r_1 = 50$ mm. The test mass $m_1 = 20$ g is mounted in any of the eight holes of the 8 surfaces in turn, and the test speed is $n_1 = 80$ r/min. The values of the two sensors are recorded during the stable rotation and data is shown in Fig. 9 after processing.

From Fig. 9, with the increase of load height, the readings of the sensor 1 remain unchanged on the whole, while the variation of the sensor 2 is proportional to the height of the testing surface, which agrees with the Eq. (17). Experimental results show the correctness of the separation principle of the horizontal vibration and the torsional vibration in the vibration mechanism, the interference by the couple unbalance is greatly reduced, and the weak centrifugal force signal is extracted from the large moment well, which provides a theoretical basis for the development of the balancing measurement system for satellite-borne rotating payload.

5.2. Detection of minimum achievable residual unbalance

5.2.1. Identification of the mount of minimum residual unbalance

The surface 2 of standard rotor R is selected as the correction-plane 1, and the test mass $m_2 = 160$ g is added to the eight angular positions of correction-plane 1 successively. The testing radius $r_2 = 75$ mm, and the working speed $n_2 = 80$ r/min. The corresponding unbalance readings of every angular position in the correction-plane 1 are shown in Fig. 10(a), where the upper dotted line corresponds to the maximum $X_{\max 1} = 233$ g and the lower dotted line corresponds to the minimum $X_{\min 1} = 89$ g. Then the minimum amount of residual unbalance is

$$U_{\mathrm{mar1}} = (X_{\max 1} - X_{\min 1})r/2 = 0.0054 \ \mathrm{kg \cdot m}$$

Similarly, the surface 6 of rotor R is selected as the correction-plane 2, so the minimum amount of residual unbalance from Fig. 10(b) is $U_{\mathrm{mar2}} = 0.00525$ kg · m.

Eq. (18) is obtained by the definition of the minimum specific unbalance e.

$$\begin{cases} U_{\mathrm{mar}} = M_{\mathrm{R}} e \\ e = \dfrac{U_{\mathrm{mar1}}}{M_1} = \dfrac{U_{\mathrm{mar2}}}{M_2} \\ M_1 + M_2 = M_{\mathrm{R}} \end{cases} \tag{18}$$

where M_1 is the corresponding mass of correction-plane 1, M_2 is the corresponding mass of correction-plane 2, then the minimum residual unbalance $U_{\mathrm{mar}} = 0.01065$ kg·m by Eq. (18).

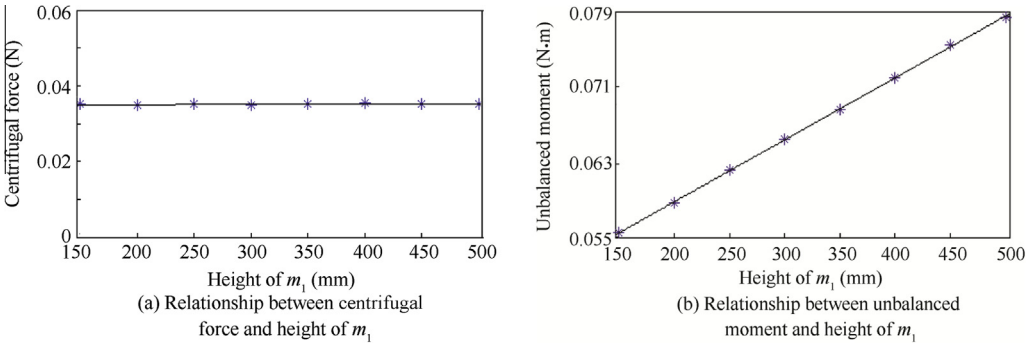

Fig. 9 Results of separation between horizontal and torsional vibration.

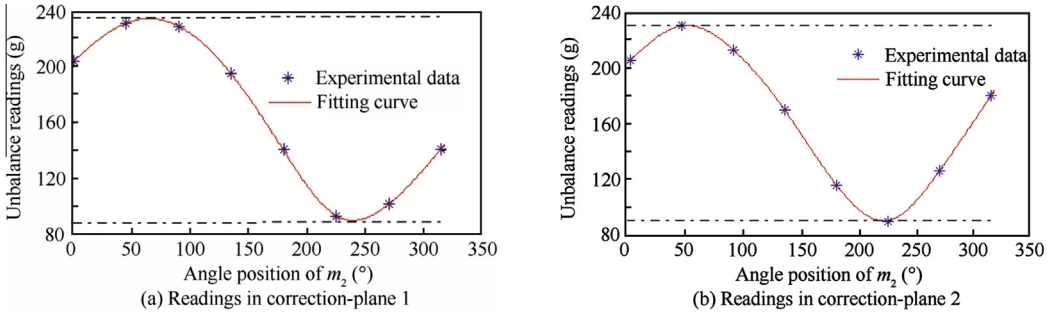

Fig. 10 Readings of two angle positions of test mass m_2.

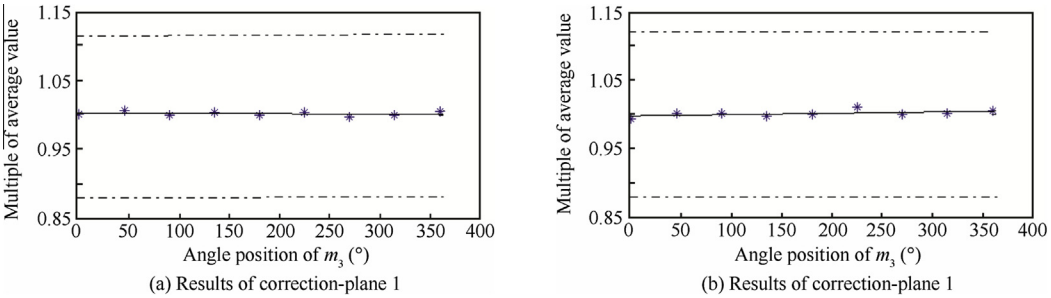

Fig. 11 Results of correction-plane 1 and 2.

Fig. 12 Practical prototype of eventually forming measurement system.

5.2.2. Detection of the minimum achievable residual unbalance

This test aims to check the claimed minimum achievable residual unbalance U_{mar} of the standard rotor by the balancing machine with the new type of vibration mechanism in terms of measurement stability. The test is carried out at the lowest speed, and balancing machine has the lowest sensitivity at the moment. For the standard testing rotor R, the minimum residual unbalance U_{mar} exists. The testing radius $r_3 = 75$ mm. The test mass should be $m_3 \in [5U_{mar}/r_3, 10U_{mar}/r_3]$ in accordance with the usual practice; however, let $m_3 = U_{mar}/r_3 = 142$ g for the standard mass is too large to fit the measurement range. The surface 6 of rotor R is selected as the correction-plane 3 and the test mass m_3 is added in turn to the eight holes of the correction-plane 3. Running the rotor R after each load, the readings of the correction-plane 1 and correction-plane 2 are recorded so that 9 pairs of data are obtained. Each reading is divided by their average of all readings of the respective plane and the results are shown in Fig. 11.

In Fig. 11, the two dotted lines (0.88 and 1.12) represent the value limits (±12%) of the arithmetic mean in each correction-plane. Known from these two figures, all plotted points are within the scope of the two dotted lines, which show a linear relationship on the whole. Thus, the balancing machine based on this vibration mechanism is able to pass the U_{mar} test, namely, with a stable balancing accuracy, it reaches the claimed minimum achievable residual unbalance.

6. Conclusions

The balancing of satellite-borne rotating payloads is very different from traditional rotors' so that it is necessary to propose new test methods and theories for dynamic balancing. A new vibration mechanism is introduced, in which the principle of the separation of the translation motion and the rotation motion is adopted in order to extract the weak centrifugal force signal from the larger overturning moment's effectively. The key issues of the low working revs and the large sizes of both the height and the centroid deviation are solved, and the defects such as poor stability and low accuracy are overcome largely. The way of determining the torsional center is used to avoid the errors aroused by the uncertainty of the vibration center. Engineering practice shows that this vibration mechanism has the superiority in the balancing for satellite-borne rotating payloads compared to other similar balancing machines, and it also has good property of mechanical separation of horizontal and torsional vibration which significantly improves the accuracy and stability of the test. After two development stages of the principle prototype and the small-scale prototype the eventually forming measurement system is shown in Fig. 12.

In order to further improve the accuracy of the weak signal at low speeds and reduce mechanical interference caused by belt drive, ultimately the techniques of air-floating and the electric spindle are developed based on the practical prototype, which are applied to the balancing detection and correction for satellite-borne rotating payloads successfully. Besides, as the satellite-borne rotors are of large size and mass, on the one hand, the supporting stability during the rotating operation is improved through the increase of the air-floating platform's size; on the other hand, the measurement system employs the electronic compensation measures to reduce or offset the errors of the vibration system aroused by the large height of the centroid deviation of the rotating antenna.

Acknowledgment

This work was supported by the National Natural Science Foundation of China (No. 51175529).

References

1. Lemmetyinen J, Kontu A, Kärnä JP, Vehviläinen J, Takala M, Pulliainen J. Correcting for the influence of frozen lakes in satellite microwave radiometer observations through application of a microwave emission model. *Remote Sens Environ* 2011;**115**(12):3695–706.
2. Matsuoka Y, Kawamura H, Sakaida F, Hosoda K. Retrieval of high-resolution sea surface temperature data for Sendai Bay, Japan, using the advanced spaceborne thermal emission and reflection radiometer (ASTER). *Remote Sens Environ* 2011;**115**(1):205–13.
3. Firth J, Black J. Vibration interaction in a multiple flywheel system. *J Sound Vib* 2012;**331**(7):1701–14.

4. Richie DJ, Lappas VJ, Prassinos G. A practical small satellite variable-speed control moment gyroscope for combined energy storage and attitude control. *Acta Astronaut* 2009;**65**(11–12):1754–64.
5. Gohary AE. Chaos and optimal control of steady-state rotation of a satellite-gyrostat on a circular orbit. *Chaos Soliton Fract* 2009;**42**(5):2842–51.
6. Aslanov V, Yudintsev V. Dynamics and chaos control of gyrostat satellite. *Chaos Soliton Fract* 2012;**45**(9–10):1100–7.
7. Green K, Champneys AR, Lieven NJ. Bifurcation analysis of an automatic dynamic balancing mechanism for eccentric rotors. *J. Sound Vib* 2006;**291**(3–5):861–81.
8. Rodrigues DJ, Champneys AR, Friswell MI, Wilson RE. Automatic two-plane balancing for rigid rotors. *Int J Nonlin Mech* 2008;**43**(6):527–41.
9. Bachschmid N, Pennacchi P, Vania A. Thermally induced vibrations due to rub in real rotors. *J. Sound Vib* 2007;**299**(4–5):683–719.
10. Ma H, Shi CY, Han QK, Wen BC. Fixed-point rubbing fault characteristic analysis of a rotor system based on contact theory. *Mech Syst Signal Pr* 2013;**38**(1):137–53.
11. Hou BF, Liu ZH, Yang JG, She WJ. Analysis to the dither in torsion coupling of low speed rotor. *Proc Eng* 2011;**16**:125–30.
12. Sève F, Andrianoely MA, Berlioz A, Dufour R, Charreyron M. Balancing of machinery with a flexible variable-speed rotor. *J Sound Vib* 2003;**264**(2):287–302.
13. Kang Y, Sheen GJ, Tang PH. The principle and applications of multi-plane separation for balancing machines. *J Sound Vib* 1997;**208**(2):167–73.
14. Saruham H. Optimum design of rotor-bearing system stability performance comparing an evolutionary algorithm versus a conventional method. *Int J Mech Sci* 2006;**48**(12):134–51.
15. Liu S, Qu L. A new field balancing method of rotor systems based on holospectrum and genetic algorithm. *Appl Soft Comput* 2008;**8**(1):446–55.
16. Lee RM, Parsons RE, inventor; Axiam Inc., assignee. Method and apparatus for geometric rotor stacking and balancing. United States patent US 7877223B2. 2011 Jan 25.
17. Warkotsch D, inventor; Horst Warkotsch Inc., assignee. Balancing device. United States patent US 6688173B1. 2004 Feb 10.
18. Royzman V, Drach I. Improving theory for automatic balancing of rotating rotors with liquid self balancers. *Mechanick* 2005;**4**(54):38–43.
19. Rajalingham C, Bhat RB. Complete balancing of a disk mounted on a vertical cantilever shaft using a two ball automatic balancer. *J Sound Vib* 2006;**290**(12):169–91.
20. Ferraris G, Andrianoely MA, Berlioz A, Dufour R. Influence of cylinder pressure on the balancing of a rotary compressor. *J Sound Vib* 2006;**292**(35):899–910.
21. Hredzak B, Guo GX. New electromechanical balancing device for active unbalance compensation. *J Sound Vib* 2006;**294**(45):737–51.
22. Wilson E, Mah RW. Automatic balancing and intelligent fault tolerance for a space-Based centrifuge. *Proceedings of the 2005 AIAA guidance, navigation, and control conference*; 2005 Aug; San Francisco, California, USA. 2005. p. 1–53.
23. Sethunadh R, Mohanlal PP. Virtual instrument based dynamic balancing system for rockets and payloads. *2007 IEEE autotestcon*; 2007 Sep 17–20; Baltimore, USA. 2007. p. 291–6
24. Brusa E, Zolfini G. Dynamics of multi-body rotors: numerical and experimental FEM analysis of the scientific earth experiment Galileo Galilei ground. *Meccanica* 2002;**37**(3):239–54.
25. Schwartz JL, Peck MA, Hall CD. Historical review of air-earing spacecraft simulators. *J Guid Control Dynam* 2003;**26**(4):513–22.
26. Wiener K, Kennedy P, Otlowski D, Rathbun B. Using a two plane spin balance instrument to balance a satellite rotor about its own bearings. *The 67th Annual Conference of Society of Allied Weight Engineers*; 2008. p. 121.
27. Li DG, Cao JG, Chen CY, Wang JW. New type of vibration structure of vertical dynamic balancing machine. *Chin J Mech Eng* 2004;**17**(4):172–82.

Wang Qiuxiao is an associate professor and master's supervisor at College of Mechanical Engineering, Chongqing University, Chongqing, China. He received the B.S. degree from Northwestern Polytechnical University in 1984, the M.S. degree from Chongqing University in 1987, and the Ph.D. degree from the same university in 2005. His research lies in the electromechanical integration technology and dynamic balancing machine.